Journal of
**Medicinal Plants and Herbs**

Research Article Open Access

# Phytochemical Profiles and Biological Activities of Glehniae Radix and its Peels

**Xiao Han, Xiao Qianru, Du Huiqing, Zheng Yi and Yuan Zhong***

School of Traditional Chinese Materia Medica, Shenyang Pharmaceutical University, Shenyang 110016, People's Republic of China

***Corresponding Author:** Zhong Yuan, Department of Analysis of Traditional Chinese Medicine, School of Traditional Chinese Materia Medica, Shenyang Pharmaceutical University, Shenyang 110016, People's Republic of China, Tel: 0086-024-4352-0715, E-mail: yuanzhong@syphu.edu.cn

**Received Date:** March 26, 2024 **Accepted Date:** April 26, 2024 **Published Date:** April 29, 2024

**Citation:** Xiao Han, Xiao Qianru, Du Huiqing, Zheng Yi, Yuan Zhong (2024) Phytochemical Profiles and Biological Activities of Glehniae Radix and its Peels. J Med Plant Herbs 3: 1-16

## Abstract

Traditional preliminary processing (TPP) is a common post-harvest procedure for Glehniae Radix cum Rhizoma (GR), characterized by the treatment of the raw roots with boiling water and then peeling off. On the market, both processed GR (pGR) and GR are available for the same medical application. In this study, the phytochemical profiles of GR, pGR, and the root peels were investigated by high-performance liquid chromatography coupled with electrospray ionization Fourier transform ion cyclotron resonance mass spectrometry (HPLC-FT-ICR-MS) method. A total of 47 phytochemicals including 27 coumarins, 11 lignan and neolignan glycosides, 2 flavonoids, 4 phenolics, and 3 polyacetylenes were tentatively identified. An HPLC method was developed for quantification of the major furanocoumarins. Compared with pGR extract, GR and the root peel extracts were more abundant with coumarins, lignans, and phenolic derivatives, especially furanocoumarin derivatives, which significantly accumulated in the root peels. Antioxidant, antiproliferative, and lipopolysaccharide-induced nitric oxide inhibitory activities of the extracts were assessed *in vitro*. GR and the root peel extracts were more effective than pGR extracts. Therefore, GR would be a better source of biologically active furanocoumarins and phenols, while the root peels as the major TPP waste have demonstrated the potential to be a novel by-product.

**Keywords**: Glehniae Radix; Traditional Preliminary Processing; Root Peels; Phytochemical Profile; Biological Activities

## 1. Introduction

Glehniae Radix (GR), commonly referred to as Beishashen in China, is the dried root of *Glehnia littoralis* Fr. Schmidt ex Miq. GR has been a *yin* tonic of traditional Chinese herbal medicine for centuries, primarily used to treat pulmonary infections and chronic bronchitis associated with dry cough [1,2]. Its medicinal value extends beyond these traditional applications, with pharmacological studies revealing GR's antioxidative [3], antimycobacterial [4], neurogenic [5], analgesic, and sedative effects [6]. The phytochemical diversity of GR is remarkable, with over 100 compounds identified, including coumarins and coumarin glycosides, lignan and neolignan glycosides, flavonoids, phenolics and phenolic glycosides, polyacetylenes, and carboline alkaloids, etc. [7-12]. These phytochemicals contribute significantly to GR's biological activities. For instance, coumarins and polyacetylenes are widely investigated phytochemicals because of their antiproliferative and inhibitory activity of nitric oxide production [13-16], while the flavonoids and phenolics are considered as the major antioxidants in GR [7]. Furthermore, the polysaccharides are abundant in GR and have been found to exhibit anticancer and anti-immunosuppressive effects [17,18].

Due to the high market demand, GR is widely cultivated in sandy soil around Inner Mongolia and the Shandong provinces of China. Traditional preliminary processing (TPP) is a crucial post-harvest procedure for GR, enhancing its drying process, improving its appearance quality, and facilitating its use in herbal preparations [2]. TPP involves removing the raw GR from the rootlet, washing and drying, processing it with boiling water for 1 minute, and then peeled off, which results in both processed GR (pGR) and GR available in the market [1].

Previous research has demonstrated that TPP significantly affects the phytochemical profile of GR. Specifically, the contents of coumarins, phenolic acids, and adenosine in GR are approximately six times higher than those in pGR [19]. This reduction in phytochemical content during TPP, particularly in the peeled-off root peels, raises the question of whether these by-products can be recycled for pharmaceutical development. Until now, there has been limited systematic investigation of the phytochemical profile and biological activities of these root peels. Additionally, information regarding the quality attributes of both GR and pGR is limited.

In this study, the phytochemical compositions of GR, pGR, and the root peels were analyzed by high-performance liquid chromatography coupled to electrospray ionization Fourier-transform ion cyclotron resonance mass spectrometry method (HPLC-FT-ICR-MS). The major furanocoumarins including xanthotoxol, marmesin, bergapten, and imperatorin were determined by HPLC method. Additionally, the antioxidant, cytotoxic, and lipopolysaccharide-induced nitric oxide inhibitory activities of GR, pGR, and the root peels were assessed. This study sought to provide critical evidence for the scientific grading of GR and pGR, while also revealing the potential of the root peels as a novel by-product with pharmaceutical value.

## 2. Materials and Methods

### 2.1. Plant Material

GR, pGR, and root peels (each 4.5 kg) were collected from Minkang planting base in Chifeng, Inner Mongolia, in September 2020, dried under shade, and then crushed into powder (40 mesh). The *G. littoralis* samples were authenticated according to the monograph for GR recorded in Chinese Pharmacopeia [1].

### 2.2 Chemicals and Reagents

Acetonitrile and methanol were HPLC-grade (Merck, Darmstadt, Germany). Distilled water was supplied by Wahaha Company (Hangzhou, China). The other used chemicals and solvents were at least analytical grade. Six reference standards (purities ≥ 98%), including bergapten, imperatorin, marmesin, scopoletin, scopolin, and xanthotoxol, were provided by Gelipu Bio-Technology Co., Ltd (Chengdu, China).

### 2.3 Sample Preparation

The 5.0 g powdered *G. littoralis* sample was extracted three times with 100 mL of 70% ethanol at an ultrasonic bath for 30 min each time. The ultrasonic conditions were as follows: power of 500 W, temperature of 30 °C. The extracting solution was evaporated under a vacuum in a ro-

tary evaporator. The residue was freeze-dried for further use.

### 2.4 HPLC-FT-ICR-MS/MS Analysis

The residue from Section 2.3 was dissolved in methanol and filtered by a microporous membrane (0.22 μm) for analysis. The chemical components were analyzed by an Agilent 1260 system equipped with a Bruker Solarix 7.0T FT-ICR MS system (Bruker, Germany). Chromatography was developed on a Kinetex C18 column (250 × 4.6 mm, 5 μm; Phenomenex, USA) at 30 °C. The mobile phase consisted of 0.1% formic acid-water (A) and acetonitrile (B) at a flow rate of 0.8 mL/min, and the chromatographic gradient program was as follows: 0–5 min, 5–20% B; 5–20 min, 20–60% B; 20–40 min, 60–90% B; 40–44 min, 90–95% B. Samples were prepared in MeOH at 5 mg/mL, and 5 μL were injected.

Mass spectrometry was operated in both positive and negative ionization modes over a mass range of 100 – 1200 Da. The electrospray ionization (ESI) source conditions were as follows: a nebulizer gas pressure of 4.0 bar, a dry gas flow rate of 8.0 L/min, a dry gas temperature of 200 °C, a capillary voltage of 4.5 kV, an end plate offset of 500 V, an ion flight time of 0.500 s, and an ion accumulation time of 0.050 s. In auto MS/MS mode, collision-induced dissociation (CID) mode was chosen, and the collision energy was adjustable from 5 eV to 25 eV according to the fragments. The mass spectra were acquired and processed by Data Analysis Software (Bruker, Germany).

### 2.5 Determination of *Xanthotoxol*, *Marmesin*, *Bergapten*, and *Imperatorin* by HPLC

The residue from Section 2.3 was dissolved in MeOH at 200 mg/mL, filtered by a microporous membrane (0.45 μm), and then 10 μL was subjected to quantitative chromatographic analysis. The chromatographic separation was performed on an LC-10AD HPLC system (Shimadzu, Japan). A Kinetex C18 column (250 × 4.6 mm, 5 μm; Phenomenex, USA) was used at 30 °C. The mobile phase consisted of water (A) and methanol (B) at a flow rate of 0.8 mL/min. A gradient elution program was set as follows: 0–3 min, 10–40% B; 3–6 min, 40–60% B; 6–15min, 60–61% B; 15–25 min, 61–62% B; 25–30 min, 62–70% B. The detection wavelength was selected at 275 nm.

#### 2.5.1 Linearity, LOD, and LOQ

The linearity and linear range were evaluated by six-point calibration curves for each standard. The detection limit (LOD) and the quantitation limit (LOQ) were determined at a signal-to-noise ratio (s/n) of 3:1 and 10:1, respectively. The noise of the baseline was analyzed by three replicate injections of 20 μL of methanol (blank). The obtained results are presented in Table 1.

#### 2.5.2 Precision and stability

To ensure the precision, the mixed standard solution was subjected to HPLC analysis by 5 times. The peak areas of xanthotoxol, marmesin, bergapten, and imperatorin were calculated for precision of quantitative analysis, and the corresponding RSD values were found less than 1.56%. Stability was tested by injecting the mixed standard solution in 0, 3, 5, 10, 15, and 30 h with RSD value less than 1.75%. The compounds stored in the dark showed stable during the tested periods at room temperature (25 °C).

#### 2.5.3 Recovery

The mixed standard solution was added in triplicate to the weighed GR sample solution, and its addition recovery was determined. The mean recoveries of the 4 standards were between 100.38% and 102.90% (Table 1).

**Table 1:** Linear regression, LOD, and LOQ of the standard compounds

| Compound | Regression equation[a] | Correlation coefficient (*r*) | Linear range (μg/mL) | LOD (μg/mL) | LOQ (μg/mL) |
|---|---|---|---|---|---|
| Xanthotoxol | $y = 35221x + 53381$ | 0.9996 | 0.25 ~ 4.00 | 0.10 | 0.35 |
| Marmesin | $y = 197101x + 23307$ | 0.9995 | 0.25 ~ 8.00 | 0.10 | 0.40 |
| Bergapten | $y = 272875x + 1614.8$ | 0.9996 | 0.20 ~ 1.80 | 0.05 | 0.18 |
| Imperatorin | $y = 158572x - 1516.2$ | 0.9996 | 0.20 ~1.10 | 0.05 | 0.17 |

[a] *x* is the concentraction of each compound in μg/mL; *y* is the peak area of the respective compound detected at 320 nm.

### 2.6 Antioxidant Assays

#### 2.6.1 1, 1-Diphenyl-2-Picrylhydrazyl (DPPH) Radical Scavenging Activity

Determination of DPPH radical scavenging activity was performed according to the method mentioned in the literature with slight modification [20]. 400 μL of DPPH (TCI Development Co., Ltd., Shanghai, China) methanol solution (60 μM) was added to 100 μL test extracts (0.1, 0.5, 1.0, 2.0, and 5.0 mg/mL) and maintainted at room temperature for 30 min. Absorbance was measured at 517 nm, with 100 μM ascorbic acid (Vc, Adamas Reagent Co., Ltd., Shanghai, China) as a positive control. The inhibitory efficiency was calculated as follows:

$$[(A_1 - A_2)/A_1] \times 100\%$$

Where $A_1$ is the absorbance of the DPPH solution and $A_2$ is the absorbance of the reacted mixture of DPPH with the extract. $IC_{50}$ value refers to the concentration of the extract required to inhibit 50% of DPPH activity.

#### 2.6.2 2, 2'-Azinobis (3-ethylbenzthiazoline-6-sulphonic acid) (ABTS) Cation Radical Scavenging Activity

ABTS cation radical ($ABTS^+$) was generated by treatment of ABTS (7 mM) with potassium persulfate (2.45 mM), as described in the literature [20]. Before using, the freshly prepared $ABTS^+$ solution was diluted with ethanol to obtain an absorbance of 0.70 ± 0.02 at 734 nm. A total of 400 μL of the $ABTS^+$ solution was mixed thoroughly with 100 μL of the sample solutions at different concentrations (0.1, 0.5, 1.0, 2.0, and 5.0 mg/mL), and kept in the dark for 15 min, then recorded at 734 nm. The scavenging activity was calculated as follows:

$$[(A_1 - A_2)/A_1] \times 100\%$$

Where $A_1$ is the absorbance of the blank without the test sample and $A_2$ is the absorbance of test samples. The scavenging activity of 100 μM ascorbic acid (Vc) was assayed as a positive control.

### 2.7 Cell Culture

Human HT-29 colon cancer cells, HL-7702 human normal liver cells and murine macrophage RAW264.7 cells were provided from Cell Resource Center (IBMS, CAMS/PUMC, Beijing, China). HT-29 cells were cultured in RPMI-1640 medium (TransGen Biotech Co., Ltd., Beijing, China), while HL-7702 cells and RAW 264.7 cells were incubated with DMEM medium (Nanjing Keygen Biotech Co., Ltd., Nanjing, China) supplemented with 10% fetal bovine serum (Nanjing Keygen Biotech Co., Ltd., Nanjing, China), antibiotic (100 units/mL penicillin and 100 μg/mL streptomycin), and 1% glutamine (v/v) under standard conditions (37°C, 5% $CO_2$).

### 2.8 MTT Assay

The antiproliferative effect of the test samples on cultured human HT-29 colon cancer cells was detected by MTT assay in 96-well microplates as described in the literature [14]. Briefly, 200 μL of adherent cells were seeded into

each well of 96-well cell culture plates, allowed to adhere for 12 h, and exposed to the test samples at concentrations of 10, 50, 100, 200, and 500 μg/mL for 72 h. Cells were re-washed and incubated for 4 h with 100 mL of MTT (1.0 mg/mL). Finally, 100 mL of DMSO was added and measured at 540 nm to determine the amount of formazan crystal. The viability of cells was quantified as a percentage compared to the control.

### 2.9 Cell Counting kit-8 Assay

Cell Counting Kit-8 (CCK-8, R&S Biotech Co., Ltd., Shanghai, China) was used to detect the antiproliferative effects of the extracts on cultured HL-7702 cells as described in the literature [21]. Briefly, 200 μL of adherent cells were seeded into each well of 96-well cell culture plates and exposed to the test samples at concentrations of 500, 200, 100, 50, and 10 μg/mL for 72 h. The absorbance at 450 nm was measured. The cell viability was quantified as a percentage compared to the control.

### 2.10 Measurement of NO

The nitric oxide (NO) production inhibitory activities of the test samples were determined as described in the literature [22]. Briefly, the cells were incubated with series concentrations (10, 20, 40, 80, 160, and 320 μg/mL) of the test samples for 4 h before stimulation with 1.0 μg/mL lipopolysaccharides (LPS, Sigma-Aldrich, St. Louis, MO, USA) for 24 h. The media were collected and assayed for NO production with a total NO assay kit (Beyotime Biotech Co., Ltd., Shanghai, China). 100 μM L-NG-Nitroarginine methyl ester (L-NAME, MultiSciences, Hangzhou, China) was used as the positive control, and inhibition (%) was calculated as follows.

$$[(A_1 - A_2)/A_1] \times 100\%$$

Where $A_1$ is the NO concentration (μM) of the LPS group, $A_2$ is the NO concentration (μM) of the mixture of the test sample and LPS group.

### 2.11 Statistical Analysis

All experiments were repeated in triplicate and the results were presented as the mean ± standard deviation (SD). Differences between groups were determined by repeated one-way analysis of variance (ANOVA) using IBM SPSS20.0 software. Statistical differences were considered significant with *P* values less than 0.05.

## 3. Results and Discussion

### 3.1 Phytochemical Profiles

To clarify the phytochemical profiles of herbal drugs, HPLC-FT-ICR-MS was employed due to its exceptional resolution and precision [23]. In this experiment, the phytochemicals of GR, pGR, and the peel samples were extracted using 70% v/v ethanol and then subjected to reversed-phase HPLC-FT-ICR-MS/MS analysis in both positive and negative modes. The typical base peak intensity chromatograms of the test samples in negative-ion mode are shown in Figure 1, which indicated that 47 chemical constituents were detected.

Based on the molecular formula determined from accurate molecular weight measurements, the generated ions from MS/MS experiment, and literature data regarding the identification of the known compounds in GR [7-11], the chemical constituents were temporarily identified and summarized in Table 2 and Figure 2. The accuracy of the identified compounds is further validated through comparing the measured mass of the compound with the theoretical mass based on its molecular formula. A good match between the two indicates a higher confidence level in the compound's identity. In detail, there were 27 coumarin and coumarin glycosides, corresponding to compounds 3, 4, 7, 8, 11, 15, 17, 18, 19, 20, 21, 23, 24, 30, 32, 33, 34, 35, 36, 37, 38, 39, 40, 41, 42, 43 and 44, 11 lignans and coumarin glycosides (compounds 5, 9, 12, 13, 14, 22, 25, 26, 27, 28, and 29), 4 phenolic acids and phenolic glycosides (compounds 1, 2, 10, 31), 2 flavonoids (compounds 6 and 16) and 3 polyacetylenes (compounds 45, 46 and 47).

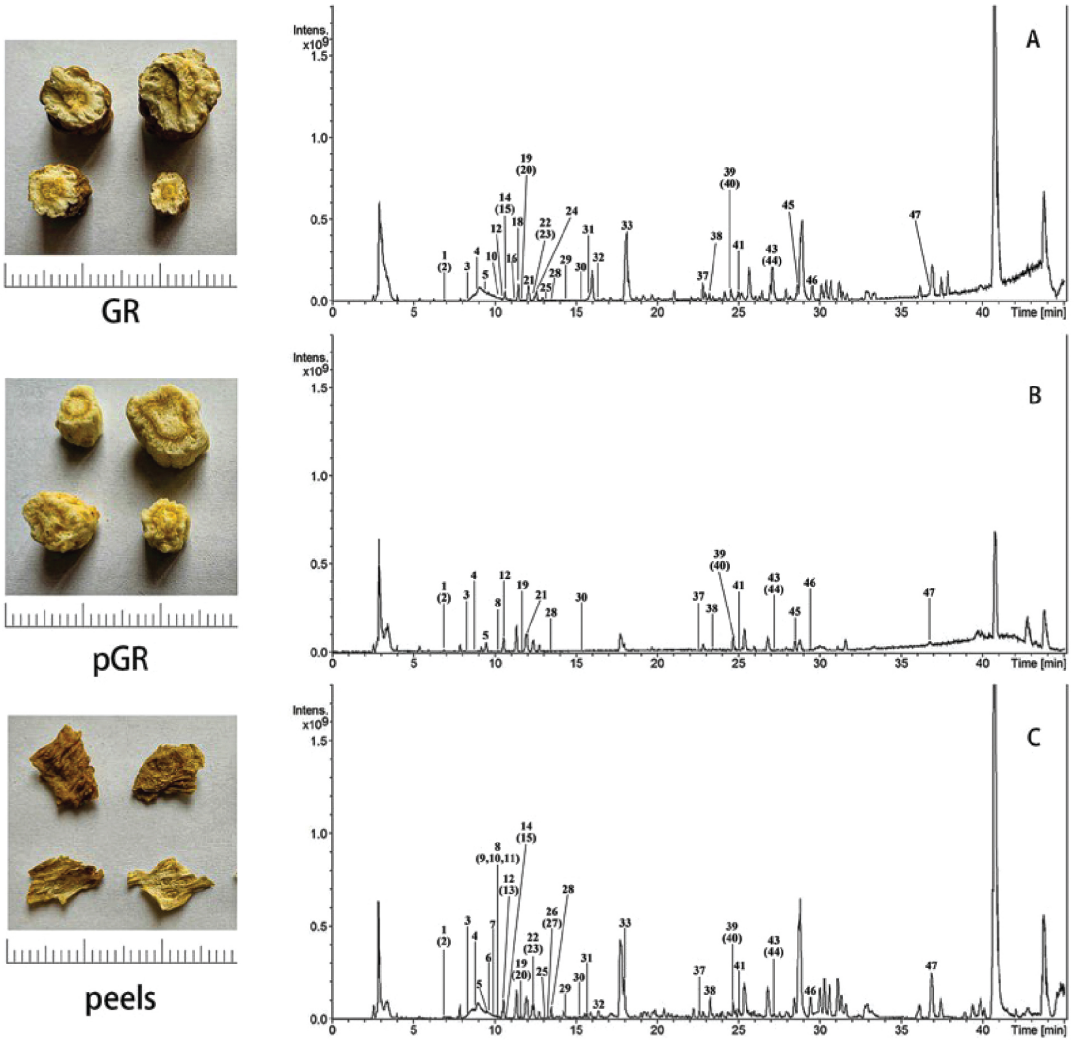


**Figure 1:** HPLC-FT-ICR MS base peak intensity chromatograms (BPCs) of the test samples in negative-ion mode. A: GR extract; B: pGR extract; C: the peels extract; the compound numbers (1- 47) are the same as those in Table 1

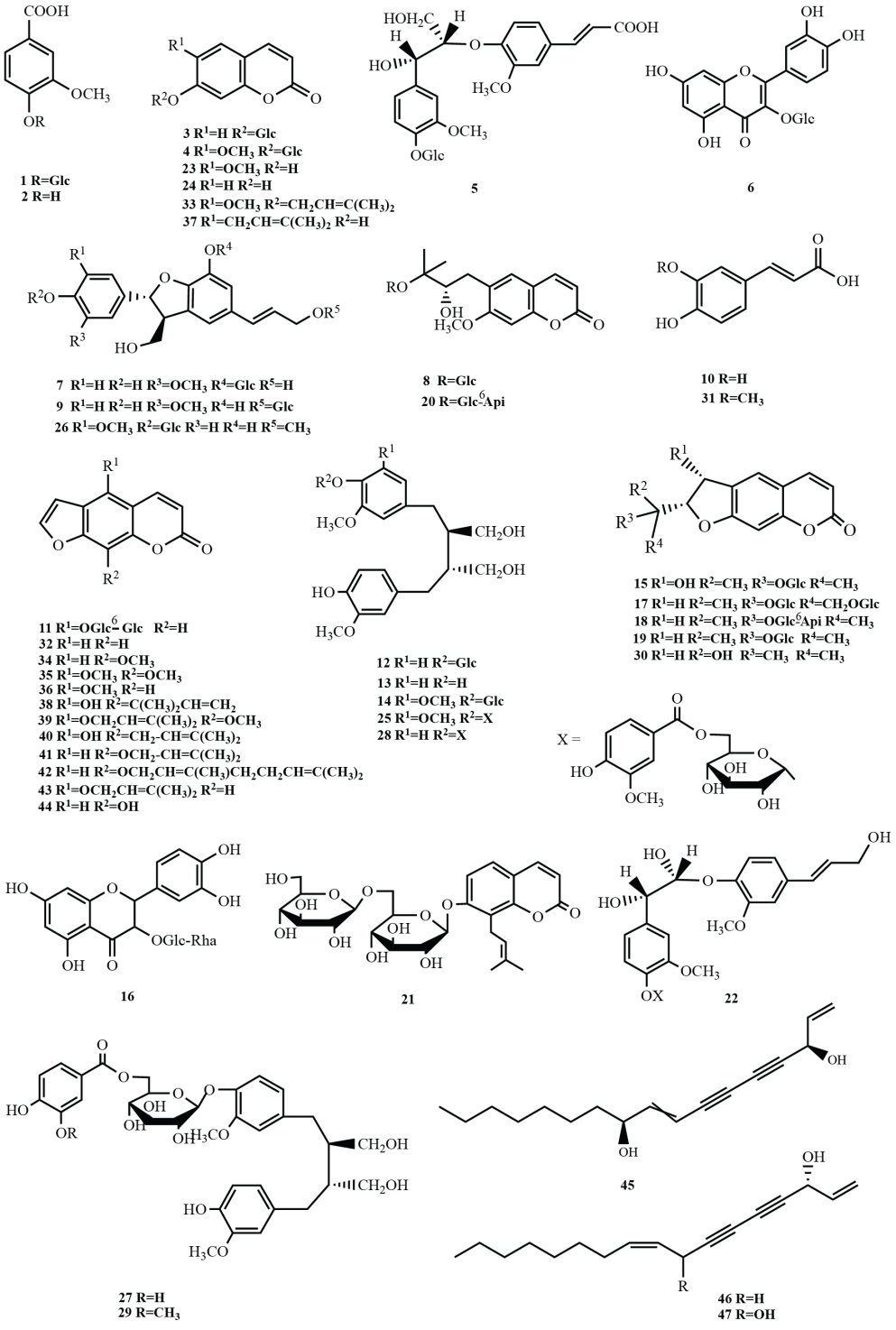


**Figure 2:** The chemical structures of detected compounds. The compound numbers (1- 47) are the same as those in Table 1; Glc: β-D-glucopyranosyl, Api: β-D-apiofuranosyl, Rha: β-D-rhamnopyranosyl

**Table 2:** The identified compounds in the test samples

| No. | $t_R$ (min) | $[M - H]^-$ | | | $[M + H]^+$ | | | MS/MS | Formula | Identification | GR | pGR | peels |
|---|---|---|---|---|---|---|---|---|---|---|---|---|---|
| | | Observed Mass (Da) | Calculated Mass (Da) | Error (ppm) | Observed Mass (Da) | Calculated Mass (Da) | Error (ppm) | | | | | | |
| **1** | 6.86 | 329.08752 | 329.08781 | 0.88 | - | - | - | - | $C_{14}H_{18}O_9$ | vanillic acid 4-*O*-β-D-glucopyranoside | + | + | + |
| **2** | 6.88 | 167.03474 | 167.03498 | 1.45 | - | - | - | - | $C_8H_8O_4$ | vanillic acid | + | + | + |
| **3** | 8.33 | 369.08211 | 369.08272 | 1.65[a] | 325.09079 | 325.09179 | 3.08 | - | $C_{15}H_{16}O_8$ | umbelliferone 7-*O*-D-glucopyranoside | + | + | + |
| **4** | 8.82 | 353.08753 | 353.08781 | 0.79 | 355.10117 | 355.10236 | 3.34 | - | $C_{16}H_{18}O_9$ | scopolin | + | + | + |
| **5** | 9.38 | 551.17674 | 551.17701 | 0.49 | - | - | - | - | $C_{26}H_{32}O_{13}$ | glehlinoside C | + | + | + |
| **6** | 9.71 | 463.08844 | 463.08820 | -0.52 | - | - | - | - | $C_{21}H_{20}O_{12}$ | isoquercetin | - | - | + |
| **7** | 9.92 | 505.17194 | 505.17154 | -0.80 | - | - | - | - | $C_{25}H_{30}O_{11}$ | 2,3-*E*-2,3-dihydro-2-(3'-methoxy-4'-hydroxy -phenyl)-3-hydroxymethyl -5-(3''-hydroxypropeyl) -7-*O*-*β*-D-glucopyranosyl -1-benzo[b]furan | - | - | + |
| **8** | 10.13 | 485.16555 | 485.16645 | 1.85[a] | - | - | - | - | $C_{21}H_{28}O_{10}$ | 7-*O*-methylpeucedanol 3' -*O*-*β*-D-glucopyranoside | + | - | + |
| **9** | 10.17 | 505.16951 | 505.17154 | 4.01 | - | - | - | - | $C_{25}H_{30}O_{11}$ | glehlinoside I | - | - | + |
| **10** | 10.18 | 179.03476 | 179.03498 | 1.24 | - | - | - | 135.04494 | $C_9H_8O_4$ | caffeic acid | + | - | + |
| **11** | 10.25 | 571.13210 | 571.13046 | -2.87[a] | - | - | - | - | $C_{23}H_{26}O_{14}$ | bergaptol 5-*O*-β -D-gentiobioside | - | - | + |
| **12** | 10.47 | 523.21772 | 523.21849 | 1.47 | - | - | - | - | $C_{26}H_{36}O_{11}$ | (–)-*seco*isolariciresinol 4-*O*-β-D-glucopyranoside | + | + | + |
| **13** | 10.48 | 361.16533 | 361.16566 | 0.92 | 363.17900 | 363.18022 | 3.34 | | $C_{20}H_{26}O_6$ | (–)-*seco*isolariciresinol | - | - | + |
| **14** | 10.56 | 553.22858 | 553.22905 | 0.85 | - | - | - | - | $C_{27}H_{38}O_{12}$ | glehlinoside G | + | - | + |
| **15** | 10.58 | 469.13496 | 469.13515 | 0.40[a] | - | - | - | - | $C_{20}H_{24}O_{10}$ | hydroxymarmesin 4'-*O*-β-D-glucopyranoside | + | - | + |
| **16** | 11.13 | 609.14574 | 609.14611 | 0.60 | - | - | - | 301.0362 | $C_{27}H_{30}O_{16}$ | rutin | + | - | - |
| **17** | 11.19 | 585.18177 | 585.18249 | 1.24 | - | - | - | - | $C_{26}H_{34}O_{15}$ | oxymarmesin 5'-*O*-β-D-glucopyranoside | - | - | + |
| **18** | 11.28 | 585.18020 | 585.18249 | 3.92[a] | - | - | - | - | $C_{25}H_{32}O_{13}$ | marmesin 4'-*O*-β-D-apiofuranosyl-(1→6) -β-D-glucopyranoside | + | - | - |
| **19** | 11.61 | 453.13985 | 453.14024 | 0.84[a] | 409.14853 | 409.14931 | 1.91 | 247.09641; 229.08590; 187.03895 | $C_{20}H_{24}O_9$ | marmesinin (nodakenin) | + | + | + |
| **20** | 11.64 | 617.20815 | 617.20871 | 0.91[a] | - | - | - | - | $C_{26}H_{36}O_{14}$ | 7-*O*-methylpeucedanol 3'-*O*-β-D-apiofuranosyl-(1→6) -β-D- glucopyranoside | + | - | + |
| **21** | 11.94 | 599.19706 | 599.19814 | 1.81[a] | - | - | - | - | $C_{26}H_{34}O_{13}$ | osthenol 7-*O*-β-D-gentiobioside | + | - | + |
| **22** | 12.34 | 687.22781 | 687.22944 | 2.37 | - | - | - | - | $C_{34}H_{40}O_{15}$ | glehlinoside D | + | - | + |
| **23** | 12.44 | 191.03474 | 191.03498 | 1.27 | 193.04931 | 193.04954 | 1.16 | - | $C_{10}H_8O_4$ | scopoletin | + | - | + |

| | | | | | | | | | | | | | |
|---|---|---|---|---|---|---|---|---|---|---|---|---|---|
| **24** | 12.58 | 161.02417 | 161.02442 | 1.53 | - | - | - | - | $C_9H_6O_3$ | umbelliferone | + | - | - |
| **25** | 13.10 | 703.25956 | 703.26074 | 1.69 | 705.27363 | 705.27530 | 2.36 | - | $C_{35}H_{44}O_{15}$ | glehlinoside B | + | - | + |
| **26** | 13.21 | 519.18677 | 519.18719 | 0.80 | - | - | - | - | $C_{26}H_{32}O_{11}$ | glehlinoside J | - | - | + |
| **27** | 13.25 | 685.24752 | 685.25018 | 3.88 | 687.26254 | 687.26473 | 3.19 | - | $C_{35}H_{42}O_{14}$ | glehlinoside F | - | - | + |
| **28** | 13.49 | 673.24896 | 673.25018 | 1.81 | 675.26304 | 675.26473 | 2.51 | - | $C_{34}H_{42}O_{14}$ | glehlinoside A | + | + | + |
| **29** | 14.38 | 699.26414 | 699.26583 | 2.41 | 701.27773 | 701.28038 | 3.78 | - | $C_{36}H_{44}O_{14}$ | glehlinoside E | + | - | + |
| **30** | 15.30 | 245.08171 | 245.08193 | 0.91 | 247.09583 | 247.09649 | 2.67 | - | $C_{14}H_{14}O_4$ | marmesin | + | + | + |
| **31** | 15.75 | 193.05036 | 193.05063 | 1.41 | - | - | - | - | $C_{10}H_{10}O_4$ | ferulic acid | + | - | + |
| **32** | 16.29 | 231.02964 | 231.02990 | 0.83[a] | - | - | - | - | $C_{11}H_6O_3$ | psoralen | + | - | + |
| **33** | 18.01 | 303.08717 | 303.08741 | 0.43[a] | - | - | - | - | $C_{15}H_{14}O_4$ | 7-*O*- (3,3-dimethylallyl) -scopoletin | + | - | + |
| **34** | 18.88 | - | - | - | 217.04921 | 217.04954 | 1.49 | 202.02555 | $C_{12}H_8O_4$ | xanthotoxin | + | + | + |
| **35** | 20.22 | - | - | - | 247.06003 | 247.06010 | 0.28 | 232.03650; 217.01304 | $C_{13}H_{10}O_5$ | isoimpinellin | + | + | + |
| **36** | 20.28 | - | - | - | 217.04944 | 217.04954 | 0.44 | 202.02604 | $C_{12}H_8O_4$ | bergapten | + | + | + |
| **37** | 22.65 | 229.08678 | 229.08702 | 1.02 | 231.10141 | 231.10157 | 0.70 | - | $C_{14}H_{14}O_3$ | demethylsuberosin | + | + | + |
| **38** | 23.25 | 269.08168 | 269.08193 | 0.60 | - | - | - | - | $C_{16}H_{14}O_4$ | 8-(1,1-dime thylallyl)-5-hydroxypsorolen | + | + | + |
| **39** | 24.57 | 299.09221 | 299.09250 | 0.96 | 301.10636 | 301.10705 | 2.29 | - | $C_{17}H_{16}O_5$ | cnidilin | + | + | + |
| **40** | 24.60 | 269.08174 | 269.08193 | 0.73 | - | - | - | 254.05898; 226.06397 | $C_{16}H_{14}O_4$ | alloisoimperatorin | + | + | + |
| **41** | 25.05 | 269.08169 | 269.08193 | 0.50 | 271.09571 | 271.09649 | 2.87 | 203.03440 | $C_{16}H_{14}O_4$ | imperatorin | + | + | + |
| **42** | 25.06 | - | - | - | 339.15904 | 339.15909 | 0.13 | - | $C_{21}H_{22}O_4$ | 8-geranyloxypsoralen | - | - | + |
| **43** | 27.09 | 269.08170 | 269.08193 | 0.86 | 271.09619 | 271.09649 | 1.09 | 203.03364 | $C_{16}H_{14}O_4$ | isoimperatorin | + | + | + |
| **44** | 27.10 | 201.01909 | 201.01933 | 1.19 | 203.03368 | 203.03389 | 0.99 | 147.04402 | $C_{11}H_6O_4$ | xanthotoxol | + | + | + |
| **45** | 28.65 | 259.17014 | 259.17035 | 0.81 | 261.18469 | 261.18491 | 0.83 | - | $C_{17}H_{24}O_2$ | panaxydiol | + | + | - |
| **46** | 29.35 | 289.18066 | 289.18092 | 0.49[a] | 245.18978 | 245.18999 | 0.88 | - | $C_{17}H_{24}O$ | panaxynol | + | + | + |
| **47** | 36.81 | 259.17010 | 259.17035 | 0.53 | 261.18492 | 261.18491 | -0.05 | - | $C_{17}H_{24}O_2$ | falcarindiol | + | + | + |

[a] m/z $[M+HCOO]^-$; + detectable; - not detectable

Among them, scopoline (4), marmesin (18), bergapten (36), imperatorin (41), scopoletin (23), and xanthotoxol (44) were accurately identified by the references. Some compounds have been analyzed in detail about their potential fragmentation patterns. By comparing them with those of known compounds, it is possible to confirm the identity of the compound. For example, compound 10 displayed a precise molecular ion at *m/z* 179.03476 $[M-H]^-$), and the molecular formula is estimated to be $C_9H_8O_4$. In its secondary mass spectrum, the fragment ion at *m/z* 135.04494 $[M-H-CO_2]^-$, which is the characteristic fragment ion of phenolic acids generated by the neutral loss of $CO_2$. Compound 10 could be tentatively identified as caffeic acid [23].

Compound 16 displayed a precise molecular ion at *m/z* 609.14574 $[M-H]^-$, and its molecular formula is estimated to be $C_{27}H_{30}O_{16}$. A neutral loss of rutinose residue generated the fragment ion $[M-H-(Rha+Glc-H_2O)]^-$ at *m/z* 301.03625. It could be speculated that compound 16 should be rutin.

Compound 19 (*m/z* 409.14853 $[M+H]^+$, $C_{20}H_{24}O_9$) released several fragment ions at *m/z* 247.09641 $[M+H-Glc]^+$, 229.08590 $[M+H-Glc-H_2O]^+$, 187.03895 $[M+H-Glc-H_2O-C_3H_6]^+$, which were formed due to the loss of glucose residue and subsequent loss of $H_2O$, $C_3H_6$.

Compound 19 might be marmesinin.

Compound 34 displayed a precise molecular ion at *m/z* 217.04921 $[M+H]^+$, and its molecular formula is estimated to be $C_{12}H_8O_4$. A neutral loss of $CH_3$ generated the fragment ion $[M+H-CH_3]^+$ at *m/z* 202.02555. It could be speculated that compound 34 should be xanthotoxin. Compound 35 (*m/z* 247.06003 $[M+H]^+$, $C_{13}H_{10}O_5$) and compound 43 (*m/z* 271.09619 $[M+H]^+$, $C_{16}H_{14}O_4$) showed the related parent ions and similar product ions to those of compound 34. Compound 35 and compound 43 were identified as isopimpinellin and isoimperatorin, respectively.

Compound 40 displayed a precise molecular ion at *m/z* 269.08174 ($[M-H]^-$), and the molecular formula is estimated to be $C_{16}H_{14}O_4$. In its secondary mass spectrum, a neutral loss of $CH_3$ generated the fragment ion $[M-H-CH_3]^-$ at *m/z* 254.05898. It continues to loss of CO to give the fragment ion $[M-H-CH_3-CO]^-$ at *m/z* 226.06397, which is the characteristic fragment ion of coumarins. Compound 40 is presumed to be alloisoimperatorin [23].

It was found that the root peels and GR extracts were more abundant with coumarin and lignan derivatives than the pGR extract. In detail, 8 types of coumarins and coumarin glycosides including 7-O-methylpeucedanol 3'-O-β-D-glucopyranoside (8), bergaptol 5-O-β-D-gentiobioside (11), oxymarmesin 5'-O-β-D-glucopyranoside (17), scopoletin (23), umbelliferone (24), psoralen (32), and 8-geranyloxypsoralen (42), and 5 types of lignans and lignan glycosides such as (–)-*seco*isolariciresinol (13), and glehlinoside I (9), D (14), G (22), and F (27) were detected in the root peels and GR extracts, which were not found in the pGR extract. In addition, the root peels and GR extracts were characterized by the presence of antioxidants including isoquercetin (6), caffeic acid (10), rutin (16), and ferulic acid (31), which were not detected in the pGR extract.

### 3.2 Furanocoumarin Content

Naturally occurring furanocoumarins, such as bergapten, imperatorin, marmesin, and xanthotoxol, showed anti-cancer [24-26], neuroprotection [27,28], anti-inflammatory [29,30], and antibacterial effects [31], while their phototoxicity and P450 enzyme inhibitory activities have also been noticed [32-34]. Furanocoumarins were proved to be the major components in GR and responsible for the similar biological activities of the herb. Therefore, a validated HPLC/UV method was developed to simultaneously determine the major furanocoumarins in GR, including xanthotoxol, marmesin, bergapten, and imperatorin (Figure 3).

HPLC analysis showed four major peaks in the chromatograms of the samples, identical with those in the chromatogram of standards and corresponding for xanthotoxol, marmesin, bergapten, and imperatorin respectively (Figure 2). As seen from the data (Table 3), the total furanocoumarin contents of GR and the root peels were 1.59- and 1.80-fold higher than that of pGR, respectively. The results indicated that the furanocoumarins mainly accumulated in the peels.

### 3.3 Antioxidant Activities

The ethanolic extracts of GR, pGR, and the peels were evaluated by $ABTS^+$ and DPPH assays for their antioxidant activities. Although the work principles are different between the two assays, the results were consistent with each other. The $IC_{50}$ value of the peel's extract was highest in both assays, and almost twice higher than that of the pGR extract (Tables 4 and 5). This may be ascribed to the fact that the antioxidants in GR such as isoquercetin, caffeic acid, rutin, and ferulic acid, greatly declined during the preliminary processing.

### 3.4 Cytotoxicity

The ethanolic extracts of GR, pGR, and the peels were evaluated against HT-29 human colon cancer cells and HL-7702 normal human liver cells for their cytotoxicity. As shown in Figure 4, all the extracts didn't affect the HL-7702 cells viability at concentrations up to 500 μg/mL. The pGR didn't demonstrate any significant antiproliferative potency, while the root peel extracts exhibited mild dose-dependent cell killing ability to HT-29 cells as compared to HL-7702 cells. The previous reports indicated that the antiproliferative activity of GR could be traceable to its furanocoumarins and polyacetylenes [13,14]. The present results, especially the pGR without any trend of antiproliferative effect, suggested that the phytochemicals responsible for the antiproliferative effects were mainly retained in the peels after the preliminary processing.

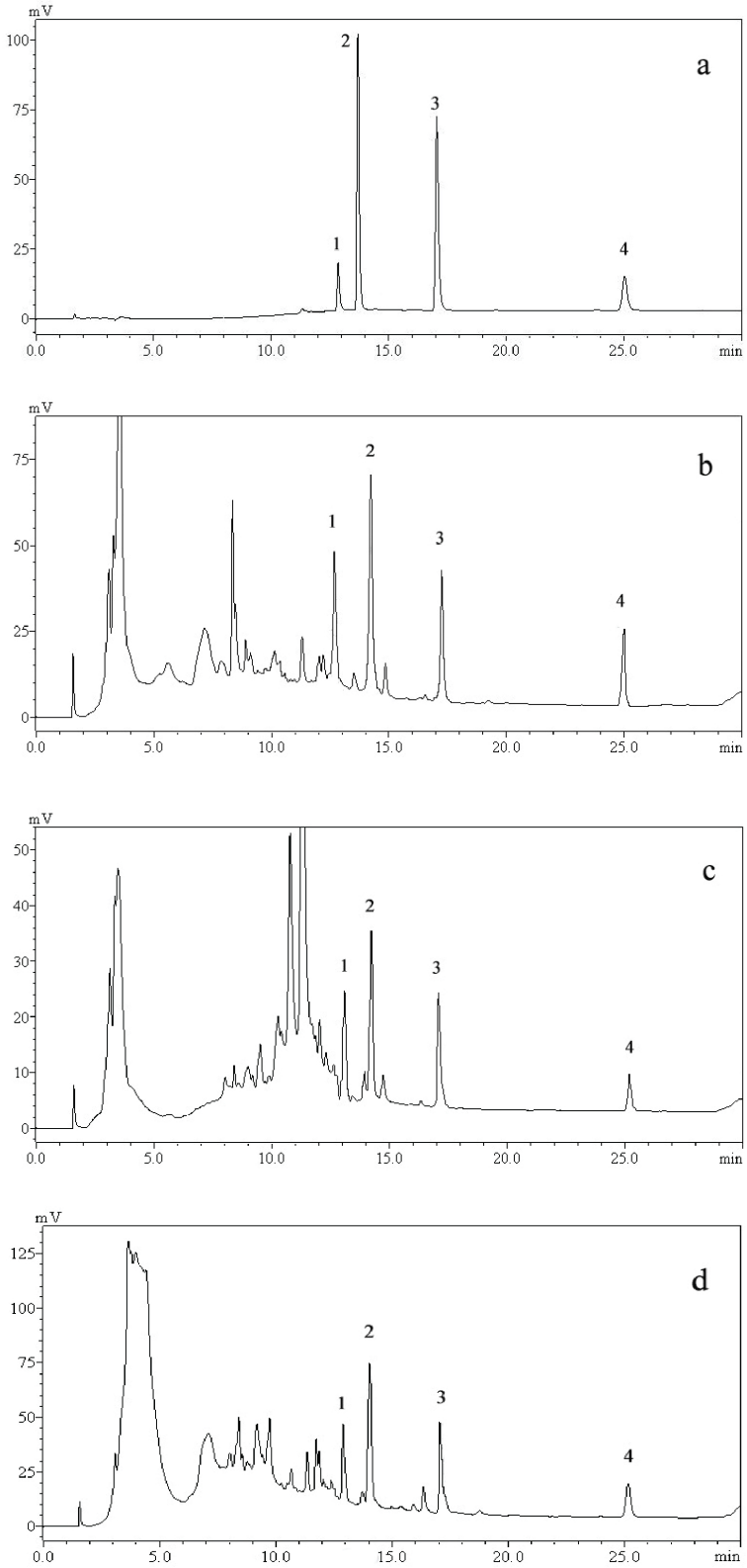


**Figure 3:** The HPLC chromatograms of the test samples. a: a mixture of standard compounds; b: GR extract; c: pGR; d: the peels extract; 1: Xanthotoxol; 2: Marmesin; 3: Bergapten; 4: Imperatorin

**Table 3:** Contents of four furanocoumarins in the test samples ($n$ = 3, mean ± SD)

| Sample | Content (μg/g) | | | | |
|---|---|---|---|---|---|
| | Xanthotoxol | Marmesin | Bergapten | Imperatorin | Total content |
| GR | 13.723 ± 0.212 | 56.689 ± 0.505 | 8.099 ± 0.282 | 10.589 ± 0.236 | 89.100 ± 0.717 |
| pGR | 8.782 ± 0.130 | 36.346 ± 0.435 | 4.314 ± 0.216 | 6.598 ± 0.286 | 56.040 ± 0.906 |
| peels | 18.403 ± 0.100 | 62.902 ± 0.197 | 7.510 ± 0.180 | 12.057 ± 0.485 | 100.872 ± 0.502 |

**Table 4:** DPPH scavenging ratios of the test samples

| Samples | DPPH scavenging ratio (%)[a] | | | | | $IC_{50}$ (μg/mL) |
|---|---|---|---|---|---|---|
| | 10 (μg/mL) | 50 (μg/mL) | 100 (μg/mL) | 200 (μg/mL) | 500 (μg/mL) | |
| GR | 14.66 ± 0.94* | 16.58 ± 1.27* | 20.91 ± 0.34* | 39.58 ± 0.53* | 57.77 ± 0.86* | 461.02 |
| pGR | 10.68 ± 0.73* | 14.04 ± 0.70* | 15.83 ± 0.84* | 17.59 ± 1.83* | 28.97 ± 2.62* | > 500 |
| peels | 14.92 ± 0.77* | 22.49 ± 2.81* | 31.25 ± 0.83* | 45.56 ± 1.00* | 65.67 ± 1.79* | 249.88 |

[a] Values represent the means ± SD in triplicates; *$P$<0.001, compared with the untreated control group

**Table 5:** $ABTS^+$ scavenging ratios of the test samples

| Samples | $ABTS^+$ scavenging ratio (%)[a] | | | | | $IC_{50}$ (μg/mL) |
|---|---|---|---|---|---|---|
| | 10 (μg/mL) | 50 (μg/mL) | 100 (μg/mL) | 200 (μg/mL) | 500 (μg/mL) | |
| GR | 4.98 ± 1.61* | 10.47 ± 0.37* | 19.48 ± 0.65* | 40.07 ± 1.07* | 75.15 ± 0.16* | 253.25 |
| pGR | 3.16 ± 1.73* | 7.52 ± 0.00* | 20.71 ± 2.27* | 35.09 ± 0.03* | 62.31 ± 0.61* | 335.47 |
| peels | 7.33 ± 1.31* | 17.94 ± 0.38* | 33.93 ± 0.91* | 57.24 ± 0.13* | 74.54 ± 0.11* | 174.66 |

[a] Values represent the means ± SD in triplicates; *$P$<0.001, compared with the untreated control group

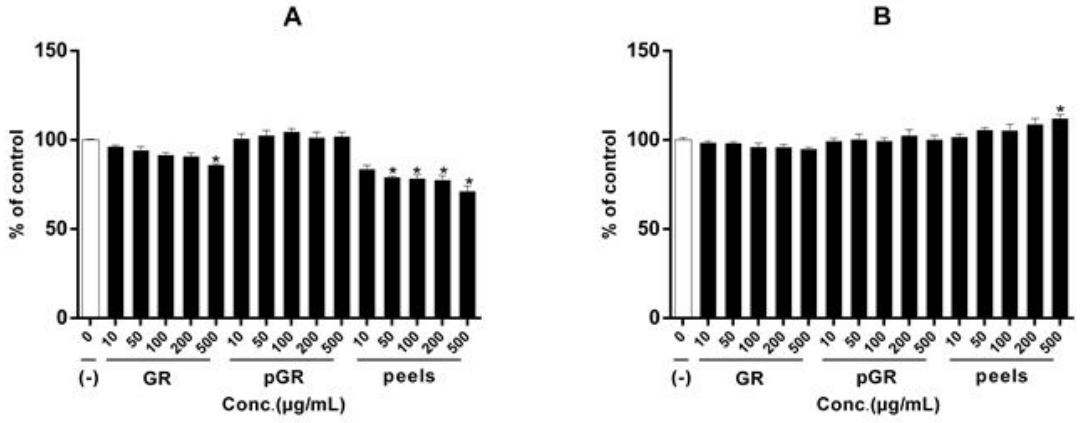


**Figure 4:** Antiproliferative effects of the test samples. A: HT-29 cellular viability; B: HL-7702 cellular viability; Results are expressed as the means ± SD of three independent experiments; *p < 0.01, compared with untreated control group

### 3.5 Lipopolysaccharide-induced Nitric Oxide Inhibitory Activities

LPS-stimulated RAW 264.7 cells were incubated with GR, pGR, and the peel extracts, and their inhibiting levels of NO were evaluated (Figure 5). The GR extract exhibited a promising dose-dependent inhibiting ability against the production of NO ($IC_{50}$ 23.14 μg/mL), similar with that of the peel extract ($IC_{50}$ 25.41 μg/mL), higher than that of the pGR extract ($IC_{50}$ 37.85 μg/mL). The present findings on the *in vitro* NO production inhibitory activities are agree with the previous findings on GR using *in vivo* models [15], moreover pyranocoumarins in GR were found to have NO production inhibitory activity [16]. Thus, the level of coumarins in GR is an important factor affecting NO production inhibitory activity, which could explain the influence of TPP on the bioactivities.

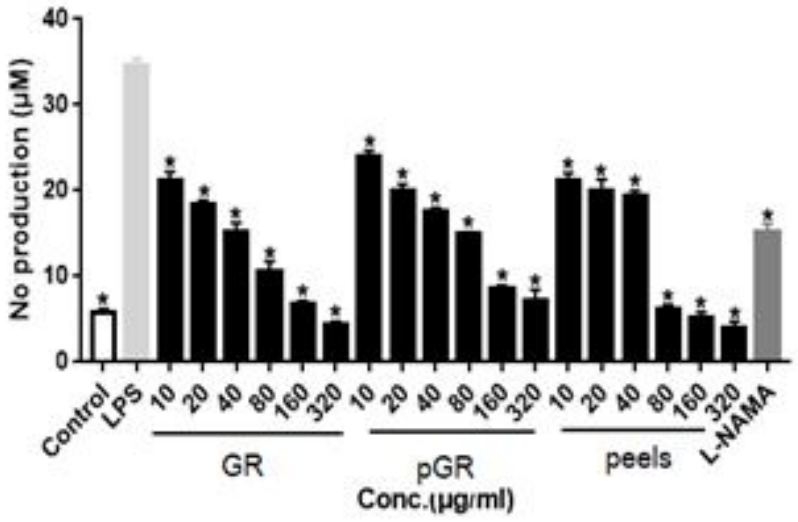


**Figure 5:** Effects of the test samples on LPS-induced NO production in RAW264.7 cells. Results are expressed as the means ± SD of three independent experiments; *p<0.001, compared with LPS group

## 3. Conclusions

The present comparative phytochemical analysis showed that GR contained higher levels of coumarin, lignan and phenolic derivatives than pGR, especially the contents of furanocoumarins in pGR samples declined significantly. Antioxidant, antiproliferative, and lipopolysaccharide-induced nitric oxide inhibitory assays revealed that GR extracts were more effective than pGR extracts. Although TPP could facilitate the drying process and improve the appearance quality of pGR, it results in the quality inconsistency of pGR in general. Moreover, a large amount of root peels was left as waste materials. For efficacious use, GR with more phytochemicals and a higher level of biological activities would be a better choice. It is expected that application of furanocoumarin or lignans as the quality markers could allow the identification of quali-quantitative differences between GR and pGR.

The present study also showed that the root peels could represent a rich source of coumarins, lignans, phenolics, flavonoids, and polyacetylenes, similar to GR in chemical composition. The peel extract demonstrated higher levels of antioxidant and anti-inflammatory activities than those of pGR extract. Furthermore, the peel extract exhibited mild dose-dependent antiproliferative effect, while the GR and pGR extracts didn't demonstrate any significant cytotoxic potency. It is worthwhile to transform the TPP waste into a novel by-product. Moreover, the therapeutic potential of the root peels deserves further exploration.

## Acknowledgments

This work was supported by the National Natural Science Foundation of China (No. 81573597).

## References


1. State Pharmacopoeia Committee (2020) Pharmacopoeia of the People's Republic of China (Part I), 1st ed. (Chinese Medicine Science and Technology Press, Beijing).

2. Jiangsu New Medical College (de.) (1977) Dictionary of Chinese Crude Drug (Part I), 1st ed. (Shanghai Scientific Technologic Publisher, Shanghai).

3. Ng TB, Liu F, Wang HX (2004) The antioxidant effects of aqueous and organic extracts of Panax quinquefolium, Panax notoginseng, Codonopsis pilosula, Pseudostellaria heterophylla, and Glehnia littoralis. J Ethnopharmacol, 93: 285-8.

4. Matsuura H, Saxena G, Farmer SW, Hancock REW, Towers GHN (1996) Antibacterial and antifungal polyine compounds from Glehnia littoralis. Planta Med, 62: 256-9.

5. Park JH, Shin BN, Ahn JH, Cho JH, Lee TK et al. (2018) Glehnia littoralis Extract Promotes Neurogenesis in the Hippocampal Dentate Gyrus of the Adult Mouse through Increasing Expressions of Brain-Derived Neurotrophic Factor and Tropomyosin-Related Kinase B. Chin Med J, 131: 689-95.

6. Okuyama E, Hasegawa T, Matsushita T, Fujimoto H, Ishibashi M et al. (1998) Analgesic components of glehnia root (Glehnia littoralis). J Nat Med, 52: 491-501.

7. Yuan Z, Tezuka Y, Fan WZ, Kadota S, Li X (2002) Constituents of the underground parts of Glehnia littoralis. Chem Pharm Bull, 50: 73-7.

8. Xu Y, Gu X, Yuan Z (2010) Lignan and neoligan glycosides from the roots of Glehnia. Littoralis. Planta Med, 76: 1706-9.

9. Liu M, Shi XW, Yang W, Liu SC, Wang N et al. (2011) Quantitative analysis of nine coumarins in rat urine and bile after oral administration of Radix Glehniae extract by high--performance liquid chromatography-electrospray ionization tandem mass spectrometry. Biomed Chromatogr, 25: 783-93.

10. Su X, Li XK, Tao HX, Zhou JE, Wu T et al. (2013) Simultaneous isolation of seven compounds from Glehnia littoralis roots by off-line overpressured layer chromatography guided by a TLC antioxidant autographic assay. J Sep Sci, 36: 3644-50.

11. Wang S, Qi PC, Zhou N, Zhao MM, Ding WJ et al. (2016) A pre-classification. Strategy based on UPLC-Triple-TOF/MS for metabolic screening and identification of Radix glehniae in rats. Anal Bioanal Chem, 408: 7423-36.

12. Zhang S, Cheng F, Yang L, Zeng J, Han F et al. (2020) Chemical constituents from Glehnia littoralis and their chemotaxonomic significance. Nat Prod Res, 34: 2822-7.

13. Kong CS, Um YR, Lee JI, Kim YA, Yea SS et al. (2010) Constituents isolated from Glehnia littoralis suppress proliferations of human cancer cells and MMP expression in HT1080 cells. Food Chem, 120: 385-94.

14. Um YR, Kong CS, Lee JI, Kim YA, Nam TJ et al. (2010) Evaluation of chemical constituents from Glehnia littoralis for antiproliferative activity against HT-29 human colon cancer cells. Process Biochem, 45: 114-9.

15. Kamino T, Shimokura T, Marita Y, Tezuka Y, Nishizawa M et al. (2016) Comparative analysis of the constituents in Saposhnikoviae Radix and Glehniae Radix cum Rhizoma by monitoring inhibitory activity on nitric oxide production. J Nat Med, 70: 253-9.

16. Lee JW, Lee C, Jin QH, Yeon ET, Lee D et al. (2014) Pyranocoumarins from Glehnia littoralis inhibit the LPS-induced NO production in macrophage RAW 264.7 cells. Bioorg Med Chem Lett, 24: 2717-9.

17. Wu J, Gao WP, Song ZY, Xiong QP, Xu YT et al. (2018) Anticancer activity of polysaccharide from Glehnia littoralis on human lung cancer cell line A549. Int J Biol Macromol, 106: 464-72.

18. Du BX, Fu YP, Wang X, Jiang HQ, Lv QT et al. (2019) Isolation, purification, structural analysis and biological activities of water-soluble polysaccharide from Glehniae radix. Int J Biol Macromol, 128: 724-31.

19. Yang W, Feng C, Kong DZ, Shi XW, Zheng XG et al. (2010) Simultaneous determination of 15 components in Radix Glehniae by high performance liquid chromatography--electrospray ionization tandem mass spectrometry. Food

Chem, 120: 886-94.

20. Zhang S, Zhang HY, Chen LX, Xia W, Zhang WQ (2016) Phytochemical profiles and antioxidant activities of different varieties of Chimonanthus Praecox. Ind Crops Prod, 85: 11-21.

21. Liu P, Zhang Y, Xu YF, Zhu XY, Xu XF et al. (2018) Three new monoterpene glycosides from oil peony seed cake. Ind Crops Prod, 111: 371-8.

22. Li JW, Wang M, Wang X, Sun L, Zhao CJ et al. (2020) Rapid characterization of the chemical constituents of Duzhong Jiangya tablet by HPLC coupled with Fourier transform ion cyclotron resonance mass spectrometry. J Sep Sci, 43: 4434-60.

23. Pattanayak SP, Bose P, Sunita P, Siddique MUM, Lapenna A (2018) Bergapten inhibits liver carcinogenesis by modulating LXR/PI3K/Akt and IDOL/LDLR pathways. Biomed Pharmacother, 108: 297-308.

24. Lv M, Xu Q, Zhang B, Yang Z, Xie J et al. (2021) Imperatorin induces autophagy and G0/G1 phase arrest via PTEN-PI3K-AKT-mTOR/p21 signaling pathway in human osteosarcoma cells in vitro and in vivo. Cancer Cell Int, 21: 689.

25. Dong L, Xu WW, Li H, Bi KH (2018) In vitro and in vivo anticancer effects of marmesin in U937 human leukemia cells are mediated via mitochondrial-mediated apoptosis, cell cycle arrest, and inhibition of cancer cell migration. Oncol Rep, 39: 597-602.

26. Sethi OP, Anand KK, Gulati OD (1992) Evaluation of xanthotoxol for central nervous system activity. J Ethnopharmacol, 36: 239-47.

27. Salem MA, Budzyńska B, Kowalczyk J, El Sayed NS, Mansour SM (2021) Tadalafil and bergapten mitigate streptozotocin-induced sporadic Alzheimer's disease in mice via modulating neuroinflammation, PI3K/Akt, Wnt/β-catenin, AMPK/mTOR signaling pathways. Toxicol Appl Pharmacol, 429: 115697.

28. Singh G, Kaur A, Kaur J, Bhatti MS, Singh P et al. (2019) Bergapten inhibits chemically induced nociceptive behavior and inflammation in mice by decreasing the expression of spinal PARP, iNOS, COX-2 and inflammatory cytokines. Inflammopharmacology, 27: 749-60.

29. Zhang HS, Ding L, Shi XQ, Mei W, Huang ZQ et al. (2021) Imperatorin alleviated NLR family pyrin domain-containing 3 inflammasome cascade-induced synovial fibrosis and synovitis in rats with knee osteoarthritis. Bioengineered, 12: 12954-64.

30. Golfakhrabadi F, Shams Ardakani MR, Saeidnia S, Akbarzadeh T, Yousefbeyk F et al. (2016) In vitro antimicrobial and acetylcholinesterase inhibitory activities of coumarins from Ferulago carduchorum. Med Chem Res, 25: 1623-9.

31. Uwaifo AO, Heidelberge C (1983) Photobiological activity of marmesin (5- hydroxyisopropyl-4, 5 dihydrofurocoumarin) in Chinese hamster V79 cells. Photochem Photobiol, 38: 395-8.

32. Wu S, Cho E, Feskanich D, Li WQ, Sun Q et al. (2015) Citrus consumption and risk of basal cell carcinoma and squamous cell carcinoma of the skin. Carcinogenesis, 36: 1162-8.

33. Wang X, Lou YJ, Wang MX, Shi YW, Xu HX et al. (2012) Furocoumarins affect hepatic cytochrome P450 and renal organic ion transporters in mice. Toxicol Lett, 209: 67-77.